Cerebral Cortex, 2021;00: 1–8

doi: 10.1093/cercor/bhaa402
Original Article

ORIGINAL ARTICLE

Chandelier Cartridge Density Is Reduced in the Prefrontal Cortex in Autism

Sarwat Amina[1], Carmen Falcone[1], Tiffany Hong[1], Marisol Wendy Wolf-Ochoa[1], Gelareh Vakilzadeh[1], Erik Allen[1], Rosalia Perez-Castro[1], Maryam Kargar[1], Stephen Noctor[2,3] and Verónica Martínez-Cerdeño[1,2]

[1]Department of Pathology and Laboratory Medicine, UC Davis School of Medicine; Institute for Pediatric Regenerative Medicine and Shriners Hospitals for Children, Sacramento, CA 95817, USA, [2]MIND Institute, UC Davis Medical Center, UC Davis School of Medicine, Sacramento, CA 95817, USA and [3]Department of Psychiatry and Behavioral Sciences, UC Davis School of Medicine, Sacramento, CA 95817, USA

Address correspondence to Verónica Martínez-Cerdeño, PhD, 2425 Stockton Boulevard; Sacramento, CA 95817, USA. Email: vmartinezcerdeno@ucdavis.edu.

Abstract

An alteration in the balance of excitation-inhibition has been proposed as a common characteristic of the cerebral cortex in autism, which may be due to an alteration in the number and/or function of the excitatory and/or inhibitory cells that form the cortical circuitry. We previously found a decreased number of the parvalbumin (PV)+ interneuron known as Chandelier (Ch) cell in the prefrontal cortex in autism. This decrease could result from a decreased number of Ch cells, but also from decreased PV protein expression by Ch cells. To further determine if Ch cell number is altered in autism, we quantified the number of Ch cells following a different approach and different patient cohort than in our previous studies. We quantified the number of Ch cell cartridges—rather than Ch cell somata—that expressed GAT1—rather than PV. Specifically, we quantified GAT1+ cartridges in prefrontal areas BA9, BA46, and BA47 of 11 cases with autism and 11 control cases. We found that the density of GAT1+ cartridges was decreased in autism in all areas and layers. Whether this alteration is cause or effect remains unclear but could result from alterations that take place during cortical prenatal and/or postnatal development.

Key words: autism, chandelier cell, cartridge, GAT1, parvalbumin, postmortem

Introduction

Autism is a neurodevelopmental condition characterized by an alteration in social communication and stereotypic/obsessive behaviors. Autism does not have a cure but can be managed through medication and therapy. Available data indicate that the cause of autism could be genetic, environmental and/or immune, but the exact cause of typical autism and other autism spectrum disorders (ASD) is not known. An alteration in the balance of excitation/inhibition has been proposed as a defining characteristic that results from a cellular and/or circuitry deficit in autism and ASD. However, little is known about the distinct excitatory and inhibitory cell populations, their molecular expression characteristics, and their function in the cerebral cortex in autism.

We previously determined that the number of parvalbumin (PV)+ Chandelier (Ch) cells is decreased in the prefrontal cortex in autism by quantifying the number of PV+ somata (Hashemi et al. 2017). Since PV is a marker for both Ch and basket cells, we distinguished between PV+ Ch and PV+ basket cells by double staining tissue with PV and *Vicia villosa* lectin (VVA) (Ariza et al.

2018). VVA binds to *N*-acetylgalactosamine that is present in the perineuronal net surrounding basket but not Ch cells. We quantified the number of PV+ somata that expressed or did not express VVA and concluded that the decreased PV+ cells we detected in the prefrontal cortex with autism corresponded to a decrease in the number of PV+ Ch cells and not PV+ basket cells (Hashemi et al. 2017; Ariza et al. 2018). Ch cells are a fast-spiking subset of PV+ GABAergic inhibitory interneurons (Szentagothai and Arbib 1974; Jones 1975) characterized by axon terminals called cartridges that are arranged perpendicular to the cortical surface and are lined with synaptic boutons (DeFelipe et al. 1985). Cartridges are rich in the Gamma aminobutyric acid (GABA) transporter 1 (GAT1)—a protein used as a specific marker of cartridges (DeFelipe and Gonzalez-Albo 1998). Ch cells are axo-axonic and synapse onto the axon initial segment (AIS) of excitatory pyramidal cells. Each pyramidal cell receives input from one or a few Ch cells (DeFelipe and Gonzalez-Albo 1998), and a single Ch cell can innervate hundreds of different pyramidal cells (Kawaguchi and Kubota 1997; Markram et al. 2004) synchronizing their activity. Thus, Ch cells directly influence cortical circuit function, and the loss of a few Ch cells can have widespread effects on circuitry and the excitation/inhibition balance. The decreased number of PV+ Ch cells that we previously described (Hashemi et al. 2017; Ariza et al. 2018) could be explained by a decreased number of Ch cells, but also by reduced or absent PV protein expression by Ch cells. Accordingly, it has been demonstrated that PV knockdown in mice, where there is no evidence of a loss of PV+ neurons, produces altered communication and repetitive and stereotyped patterns of behavior (Vreugdenhil et al. 2003; Schwaller et al. 2004; Wohr et al. 2015). PV plays a role in short-term synaptic plasticity and in PV knockout mice synapses with short-term depression are converted to synapses with short-term facilitation resulting in enhanced synaptic transmission (Caillard et al. 2000). Therefore, while a loss of Ch cells would decrease inhibition, downregulation of PV would lead to increased inhibition. However, both, a decrease in the number of Ch cells or a decreased PV expression by Ch cells, would alter pyramidal neuron inhibition and consequently synaptic transmission in the autistic cerebral cortex.

To further test our previous result demonstrating a decrease of PV+ Ch cell number, we quantified Ch cell number following a different approach and using a different patient cohort of cases than used in our previous studies. Specifically, we quantified the number GAT1+ cartridges—rather than PV+ Ch cell somata—per radial length of cortex (density), in supragranular and infragranular layers of prefrontal Broadman areas (BA)9, BA46, and BA47. The data obtained in this study provide additional data supporting a decrease in the number of Ch cells in the prefrontal cortex in autism.

Materials and Methods

Samples

Postmortem human tissue from 11 cases with autism and 11 control cases matched for age and sex was obtained from the Autism Tissue Program, NIH Neurobiobank, and UC Davis FXS/FXTAS brain repository (node of the Hispano-American Brain Bank on Neurodevelopmental Disorders (CENE)) (Table 1). The average age of cases with autism was 15.36 years, with a range of 7–23 years. The average age of control cases was 15.72 years, with a range of 7–24 years. The average postmortem interval (PMI) was 19 for autism, and 19.95 for control. Autism diagnoses were confirmed by respective brain banks through standard postmortem use of the Autism Diagnostic Interview-Revised (ADI-R) or through record review. Control cases were defined as free of neurological disorders based on medical records and information gathered at the time of death from next of kin. Two of the subjects with autism suffered from seizures, 4 suffered from intellectual delay, one presented with bipolar disorder, and other from intermittent explosive disorder. For causes of death see Table 1. Prefrontal cortex areas BA9, BA46, and BA47 were isolated based on Brodmann anatomy as we previously described (Hashemi et al. 2017). Tissue blocks were fixed in 10% buffered formalin, cryoprotected in a 30% sucrose solution in 0.1 M phosphate-buffered saline with 0.1% sodium azide. Tissue was embedded in optimum cutting temperature compound, and frozen at −80 °C. A cryostat was used to cut 14 µm-thick slide-mounted sections, stored at −80 °C until use.

Anatomical and Cytoarchitectural Considerations

We used Brodmann cortical neuroanatomy to isolate a block containing area BA9 in the superior frontal gyrus, BA46 in the middle frontal gyrus, and BA47 in the inferior frontal gyrus, from each case (Fig. 1). One section per case was Nissl-stained and used to confirm cortical areas based on von Economo histology as previously described (Hashemi et al. 2017). Adjacent sections were used for immunostaining. Summarizing, BA9 (magnocellular "granular frontal area," or F_{Dm} of von Economo) consists of a strip-like zone whose medial boundary is the callosomarginal sulcus and its ventral boundary is the inferior frontal sulcus, including the anterior half of the superior frontal gyrus and the posterior third of the middle frontal gyrus. BA46 ("middle granular frontal area," or $F_{D\Delta}$ of von Economo) includes the previous two-thirds of the middle frontal gyrus and the most anterior part of the inferior frontal gyrus at the transition to the orbital surface. BA47 ("orbital area" or $F_{F}\alpha$ of von Economo) surrounds the posterior branches of the orbital sulcus, and laterally crosses the orbital part of the inferior frontal gyrus. Layers III and V exhibit a clear sublamination in BA9, but not in BA46. Neurons in BA46 are more homogeneous in size than those in BA9. BA9 is characterized by the presence of large pyramidal cells in sublayers IIIc and Va1, a pale violet-stained sublayer Vb, and a narrow and indistinct layer IV. BA46 is characterized by relatively low cell-packing density and a violet-pale sublayer Vb. BA47 has a higher cell density in layer Vb and small and medium pyramidal cells in layer IIIc (Von Economo and Koskinas 1928).

Immunostaining

Sections were immunostained with antibody against GAT1. Briefly, tissue was treated with 1:1 chloroform:100% ethanol followed by sequential immersion in EtOHs and deionized water. Antigen retrieval was performed by exposing the tissue to 110 °C for 8 min. in TBS, and slides were washed with TBS twice followed by TBS + 0.05% tween once. Endogenous peroxidase blocking was performed with 3% H_2O_2. The slides were blocked with 1X TBS + 10% Normal donkey serum +0.02% triton for 1 h at room temperature, and then treated with an avidin-biotin blocking kit (Vector Labs). Primary antibody solution polyclonal rabbit anti-GAT1 (1:250, Abcam) was added for 24 h at 4°C with Parafilm coverslips in a dark humidified box. Slides were washed and incubated with the secondary antibody, donkey anti-rabbit conjugated with biotin (1:200, Abcam) for 1 h, washed, and incubated with 500 µL ABC solution (Vector Labs) for 2 h. After

Table 1 Characteristics of cases included in this study

Case	Diagnosis	Age (years)	Sex	PMI	Cause of death
4203	Control	7	Male	24	Respiratory insufficiency
4337	Control	8	Male	16	Accident
5554	Control	13	Female	15	Suicide
5309	Control	14	Female	8	Infection
5834	Control	14	Male	38	Cardiac failure
4638	Control	15	Female	5	Accident
AN07444	Control	17	Male	NK	Aphyxia
5893	Control	19	Male	11	Cardiac failure
5646	Control	20	Female	23	Reactive airway disease
5958	Control	22	Male	24	Cardiac failure
AN01891	Control	24	Male	35	NK
5144	Autism	7	Male	3	Cancer
AN03221	Autism	7	Male	NK	Drowning
4305	Autism	12	Male	13	Serotonin syndrome
AN00754	Autism	13	Male	NK	SUDEP
4899	Autism	14	Male	9	Drowning
AN02736	Autism	15	Male	NK	Aspiration
5403	Autism	16	Male	35	Cardiac failure
4269	Autism	19	Male	45	Meningitis
4999	Autism	20	Male	14	Cardiac failure
5176	Autism	22	Male	18	Subdural hemorrhage
5574	Autism	23	Male	14	Pneumonia

washing, slides were developed with DAB substrate (brown; Vector Labs) and washed. Tissue was dehydrated through sequential immersion in EtOHs for 5 min. Each, then cleared in Xylene for 10 min., and coverslipped with Permount mounting medium.

Quantification

Specific regions of the cerebral cortex cannot be delineated, and therefore stereology cannot be applied. Instead, we quantified each single cartridge within a selected region within each area of interest (density). This region spanned a 3-mm wide bin parallel to the ventricular surface that extended perpendicular from the pia through the thickness of the cortical gray matter to include all cortical layers. GAT1+ cartridges were identified based in their brown color and typical morphology under a 100X oil objective and plotted and quantified using StereoInvestigator Software (Olympus BX61 microscope with a Hamamatsu Camera, a Dell Precision PWS 690, Intel Xeon CPU Computer with Microsoft Windows XP Professional V. 2002 system and MBF Bioscience StereoInvestigator V.9 Software, MicroBrightField, Williston, VT). We performed replication studies in a second 3-mm bin selected from a different region within each cortical area.

Statistics

The goal of the statistical analysis was to compare the number of cartridges between autism and control cases in each area, and to assess the relationship between anatomical parameters and other patient/sample characteristics (such as age, PMI, and time in formalin). Each variable was compared between autism and control cases using *t*-tests. The joint influence of autism and patient/sample characteristics on variables was assessed with an analysis of covariance. SPSS 26 (IBM) was used for statistical analyses, and graphs were generated with Prism 6 (GraphPad). Statistical significance was set at $a < 0.05$.

Results

We obtained tissue from 11 autism and 11 control cases. Diagnosis, age, sex, PMI, and cause of death are included in Table 1. Within each area of interest (BA9, BA46, and BA47), we chose a 3-mm wide bin that extended from the pial surface through the thickness of the gray matter to include all cortical layers (Hashemi et al. 2017). To ensure that we obtained representative samples of cartridges in each area, we performed replication studies in a second 3-mm bin selected from a different region within each cortical area.

We labeled cartridges through enzymatic immunochemistry with an antibody against GAT1 in sections that were adjacent to those in which we performed Nissl. The cortex presented with a multitude of GAT1+ puncta that were distributed throughout all layers. GAT1 immunostaining delineated neuronal somata, processes, and cartridges (Fig. 2). Cartridges were arranged perpendicular to the cortical surface, measured 20–40 µm in length, and were populated by synaptic boutons. We quantified GAT1+ cartridges in prefrontal areas BA9, BA46, and BA47, and built a representation of the cartridge population for each area. A representative example of GAT1+ cartridges in autism and control cases in each of the 3 areas of interest is shown in Figure 3.

We found that the total number of GAT1+ cartridges was decreased in autism cases when compared with the control cases (Fig. 4). This decrease was of 39% ($P = 0.002$) in BA9, (1871.3 ± 150.8 in control, 1106.4 ± 116.05 in autism); of 61% ($P = 0.004$) in area BA46 (1560.2 ± 253.1 cartridges in control, 616.6 ± 101.0 in autism); and of 46% ($P = 0.02$) in BA47 (1792.0 ± 302.7 in control, 980.6 ± 96.3 in autism).

The average number of cartridges was 1048 ± 103.1 in control and 685.1 ± 78.1 in autism in supragranular layers of BA9 ($P = 0.03$); 823.8 ± 126.1 in control and 316.4 ± 50.5 in autism in supragranular layers of BA46 ($P = 0.002$); and 936.1 ± 135.0 in control and 584.1 ± 61.6 in autism in supragranular layers of BA47 ($P = 0.04$).

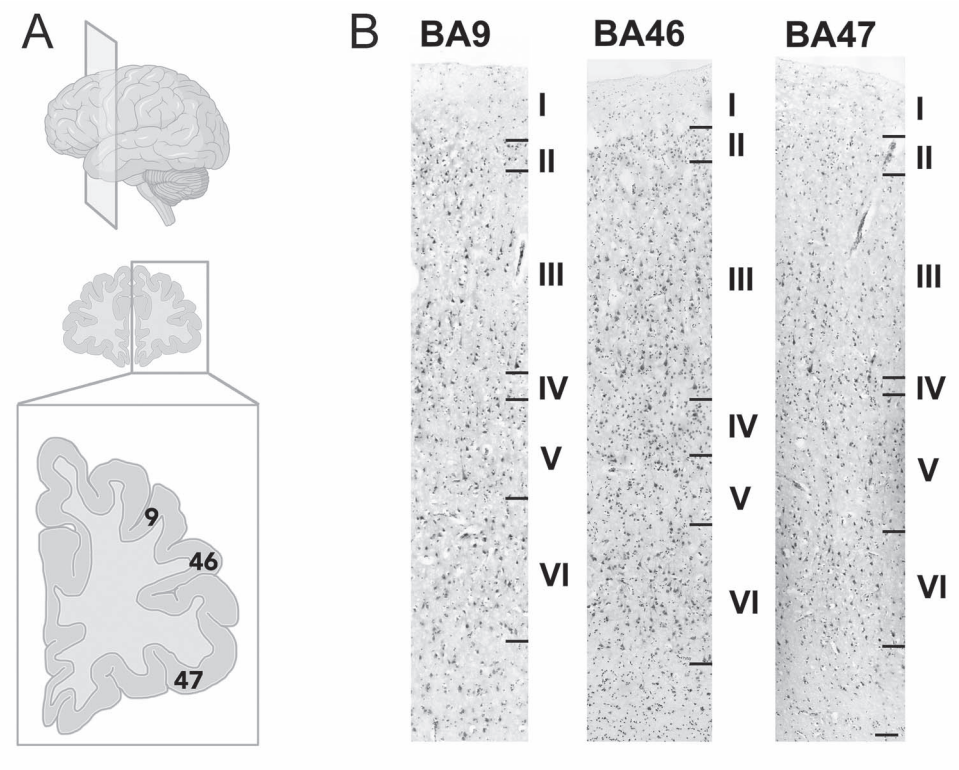

Figure 1. (*A*) Prefrontal regions selected for this study: BA9, BA46, and BA47. (*B*) Nissl-stained columns of the prefrontal regions of interest. Scale bar: 300 µm.

The average number of cartridges was 824.63 ± 91.5 in control and 413.3 ± 69.9 in autism in the infragranular layers of BA9 ($P = 0.002$); 740.9 ± 137.9 in control and 300 ± 57.3 in autism in the infragranular layers of BA46 ($P = 0.01$); and 835.9 ± 186.5 in control and 396.55 ± 45.7 in autism in the infragranular layers of BA47 ($P = 0.04$).

These data indicate a decreased in GAT1+ cartridges in both upper and lower layers present in the 3 prefrontal areas of interest (BA9: 35% ($P = 0.033$) decreased in supra vs. 50% ($P = 0.002$) in infragranular; BA46: 61% ($P = 0.002$) decreased in supra vs. 60% ($P = 0.012$) in infragranular layers; BA47; and 38% ($P = 0.048$) decreased in supra vs. 53% in infragranular ($P = 0.041$)).

Overall, we found a generalized decrease in the number of GAT1+ cartridges in the prefrontal cortex in autism when compare with control cases. No statistically significant influence of covariates was found, including for age and PMI in the areas analyzed ($P > 0.05$).

Discussion

The Number of Ch Cells Is Decreased in the Prefrontal Cortex in Autism

We quantified the number of GAT1+ cartridges within the area of interest (density) in the prefrontal cortex and found a decreased number in autism when compared with control cases. The decrease in the number of GAT1+ cartridges was of 39% in BA9, 61% in BA46, and 42% BA47. These data matched data obtained in our previous quantification studies that examined the number of PV+ somata in the cortex in autism. In our previous work we classified interneurons into 3 subpopulations based on expression of the calcium-binding proteins PV, calbindin (CB), and calretinin (CR), and quantified the number of each interneuron subtype in postmortem prefrontal tissue from 11 cases with autism and 10 control cases. We found that the number of PV+ interneurons was significantly reduced in autism compared with controls cases, whereas the number of CB+ and CR+ interneurons did not differ (Hashemi et al. 2017). Our previous work also demonstrated that most, if not all, of the decrease in PV+ cells was due to a decrease in PV+ Ch cells, with very little involvement of PV+ basket cells (Ariza et al. 2018). We reported a decrease in interneuron ratio for PV+ somata of 45% in BA9, 70% in BA46, and by 38% in BA47 (Hashemi et al. 2017). We also obtained the total number of PV+ somata per area (the same 3-mm wide bins), and found a decrease of PV+ somata of 42% in BA9, 60% in BA46, and by 31% in BA47. When we compared the total number of cartridges to the total number of PV+ somata we found striking similarity (39% GAT1+ cartridges vs. 42% PV+ somata in BA9; 61% and 60% in BA46; and 46% vs. 31% in BA47). That both data sets came to similar findings using different methodology—different cell markers and cell structures labeled in a different cohort of patients, corroborates the finding that the number of Ch cells is decreased in prefrontal cortical areas in autism. These data also suggest that the decrease in PV+ somata we found in our previous study was not due to a decrease in PV protein expression by Ch cells, but rather to a decrease in the number of Ch cells. In addition, it also suggest that each of the remaining Ch cells contains the same number of cartridges. We found that both upper and lower layers presented with a decreased in GAT1+ cartridges in the 3 prefrontal areas of interest, also in agreement our data on PV+ somata.

The slight variation in the number of each component (PV+ somata vs. GAT1+ cardtriges) could result from the different set

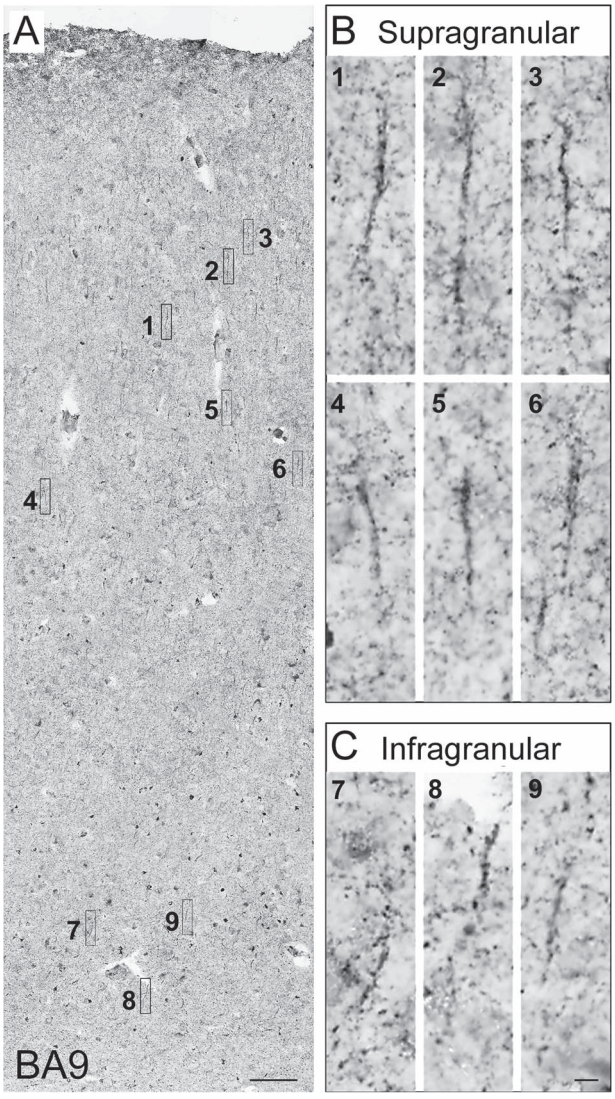

Figure 2. (*A*) GAT1 immunostaining of BA9 prefrontal cortex in a control case. (*B* and *C*) High magnification of cartridges outlines in A, located in upper (*B*) and lower (*C*) layers. Scale bar: 500 µm in (*A*), 25 µm in (*B*).

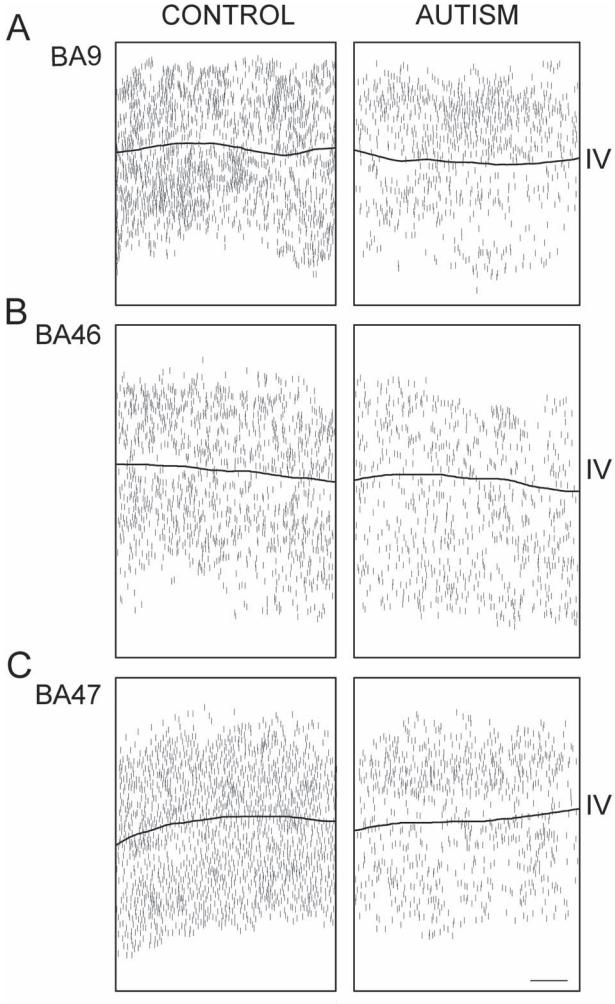

Figure 3. Representation of the average cartridge distribution within cortical areas BA9 (*A*), BA46 (*B*), and BA47 (*C*) for control and autism cases. Cases of autism have less cartridges that control cases for the same area. Scale bar: 500 µm.

of cases included in these studies. Cases included in the current studies were younger (children and adolescents) than in the previous study (children, adolescents, and adults). Accordingly, it has been shown that the density of GAT1+ cartridges changes with age in human and monkey (DeFelipe et al. 1985; DeFelipe and Gonzalez-Albo 1998; Cruz et al. 2003; Pakkenberg et al. 2003).

The decreased in inhibitory Ch cells may translate into a lack of inhibitory signal into the proximal axon of the excitatory pyramidal cell, and this may result in a hyperexcitation of the cortical output. However, other variables such as the number of synaptic boutons per cartridge/Ch cell, the amount of GABA release by Ch cells, and Ch cell level of activity, need to be taken into account in order to understand how this change in Ch cells number affects the function of the cortical circuitry in autism.

There Is a Lower Number of Ch Cells in BA46 Than Other Prefrontal Areas

The data obtained from control cases presented here indicate that while BA47 and BA9 present similar number of cartridges, BA46 has a lower number of cartridges (14% less than BA47 and 19% less than BA9). These data agree with our previous data on the number of PV+ cells in human, and with other data demonstrating a heterogenous number of Ch cells across cortical areas in human and other mammals. The abundance of cartridges has been correlated with a higher proportion of pyramidal cells in a given cortical area and species (DeFelipe and Gonzalez-Albo 1998). Primary and secondary sensory cortical areas in human have a lower density of Ch cells compared with other areas. Motor and associative fronto-lateral areas show a 2-fold increase in the number of Ch cells compared with sensory areas, and frontal, associative temporal areas, and cingulate areas present a 3-fold increase in the number of Ch cells, compared with sensory areas. There are also differences in the number of cartridges per layer, with the lowest density of cartridges in infragranular layers, and the highest density of cartridges in supragranular layers (Arellano et al. 2002). These differences in the number of cartridges among the cortical areas and layers likely correlate to different functional attributes associated with each specific cortical region or layer.

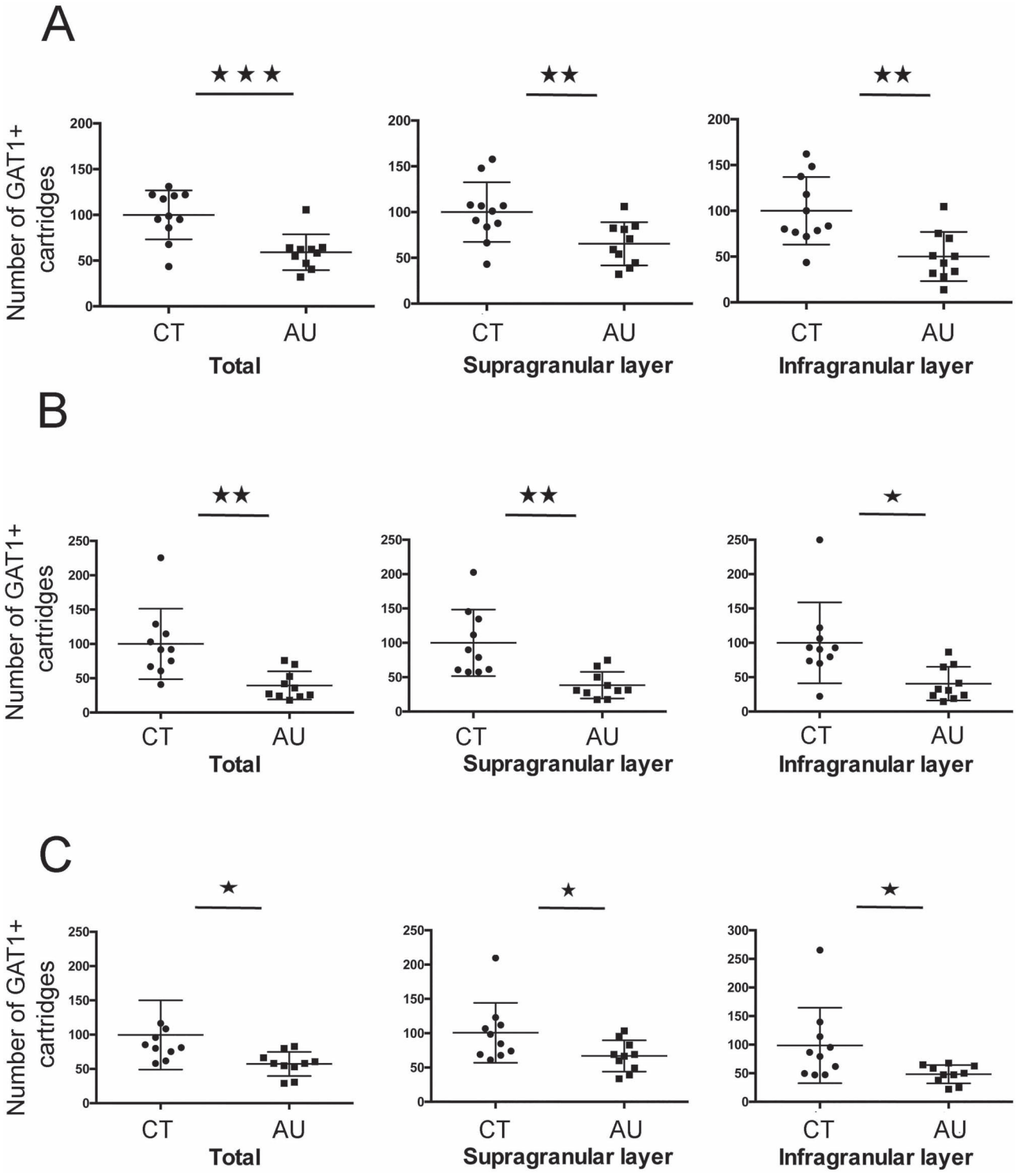

Figure 4. Number of cartridges in the whole radial dimension (total), supragranular layers, and infragranular layers, in the cerebral cortex in control and autism cases in BA9 (*A*), BA46 (*B*), and BA47 (*C*). There is a significant decrease in the number of cartridges in all cases. Horizontal bar represents the mean and whiskers the standard deviations.

The Decrease in the Number of Ch Cells in the Cortex Most Likely Arise from Prenatal and/or Postnatal Events

PV+ cells are generated during prenatal development in the medial ganglionic eminence (MGE) and the preoptic area (POA) from progenitor cells that express the transcription factor NKX2.1 (Sussel et al. 1999; Xu et al. 2008; Fazzari et al. 2010). In mouse Ch cells are generated in the ventral region of the MGE between E12 and E17 (Inan et al. 2012; Taniguchi et al. 2013; Sultan et al. 2018). Once generated new-born cells migrate

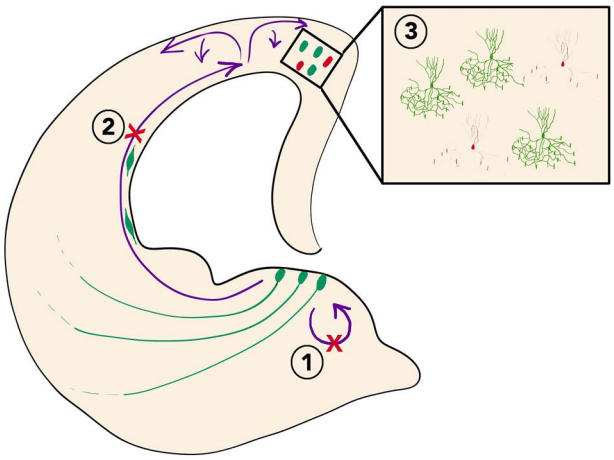

Figure 5. An alteration in the process of generation (1), migration (2), and/or cell death (3) could be responsible for the decreased number of Ch cells that we described in autism.

from the MGE tangentially into the cortex along the wall of the ventricle, reaching the cortex at E18-P0. Upon reaching dorsal cortex the migrating cells split into medial, lateral, and anterior migratory streams that populate the cortical SVZ by P1, and turn radially to cross the cortical plate, reaching layer I at P2-3, where they continue to spread for several days before descending back into the cortex (Taniguchi et al. 2013). Once in the cerebral cortex, they mature and acquire their final morphology, connectivity, and activity pattern. Any alteration in the processes of generation, cell death, and migration into their final cortical location, that occur during prenatal and postnatal development, could be responsible for the decreased number of Ch cells that we identified in autism (Fig. 5). Other events, such as failure in proper integration and refinement into circuits, and/or establishment of characteristic activity patterns could be responsible for dysfunction of Ch cells (Southwell et al. 2012; Denaxa et al. 2018; Lim et al. 2018; Wong et al. 2018).

Autism does not have a characteristic pathology but the scarce data available concerning neuropathology found in autism supports an alteration that occurs during development. The most notable publication on the pathology of autism is that by Wegiel et al. (2010), which described a broad spectrum of focal neuropathological changes in 12 of 13 brains of autistic subjects. Alterations in neurogenesis are supported by the thickening of the subependymal cell layer that was present in 2 of the cases included in Wegiel study, whereas migratory alterations are supported by the present of frequent heterotopias detected in 4 of those brains, specifically periventricular heterotopias that could result from failures of neuronal migration (see Fig. 5). Future studies should investigate the incidence of periventricular heterotopias in broader samples of autistic cases, and whether the heterotopias are composed by new-born interneurons, including those fated to be Ch cells. An altered number of Ch cells could also result from increased cell death. For example, once Ch cells complete migration and reach their final destination in the cortex, they may exhibit an increased rate of cell death before or after they mature (Figs 3–5). White matter pathology that we have observed in ASD, specifically pencil fibers in the prefrontal cortex, could also reflect defects in neuronal migration (Hashemi et al. 2017). Dysplasia are also found in the brain with autism however this are most likely failure in the maturation cell programs and the capacity of the newborn cells to integrate within the circuitry.

Conclusion

We conclude that the number of cartridges and Ch cells is decreased in the prefrontal cortex in autism. Additional studies will be needed to determine if the number of Ch cells is affected in other cortical areas. A decrease number of Ch cells in the cortical circuitry could translate into a hyperexcitation of signal output from cortical circuits. However, whether the altered number of Ch cells in autism is a primary cause of altered circuitry, or a downstream effect of underlying pathology remains unclear. Future studies will shed light on the cause of decrease number of Ch cells in the cerebral cortex with autism.

Funding

The National Institute of Mental Health (NIMH, R01MH094681); Medical Investigation of Neurodevelopmental Disorders (MIND) Institute (IDDRC; U54HD079125); ARTP (Autism Training Program) at the MIND Institute; and Shriners Hospitals.

References

Arellano JI, DeFelipe J, Munoz A. 2002. PSA-NCAM immunoreactivity in chandelier cell axon terminals of the human temporal cortex. *Cereb Cortex*. 12:617–624.

Ariza J, Rogers H, Hashemi E, Noctor SC, Martinez-Cerdeno V. 2018. The number of chandelier and basket cells are differentially decreased in prefrontal cortex in autism. *Cereb Cortex*. 28:411–420.

Caillard O, Moreno H, Schwaller B, Llano I, Celio MR, Marty A. 2000. Role of the calcium-binding protein parvalbumin in short-term synaptic plasticity. *Proc Natl Acad Sci USA*. 97:13372–13377.

Cruz DA, Eggan SM, Lewis DA. 2003. Postnatal development of pre- and postsynaptic GABA markers at chandelier cell connections with pyramidal neurons in monkey prefrontal cortex. *J Comp Neurol*. 465:385–400.

DeFelipe J, Gonzalez-Albo MC. 1998. Chandelier cell axons are immunoreactive for GAT-1 in the human neocortex. *Neuroreport*. 9:467–470.

DeFelipe J, Hendry SH, Jones EG, Schmechel D. 1985. Variability in the terminations of GABAergic chandelier cell axons on initial segments of pyramidal cell axons in the monkey sensory-motor cortex. *J Comp Neurol*. 231:364–384.

Denaxa M, Neves G, Burrone J, Pachnis V. 2018. Homeostatic regulation of interneuron apoptosis during cortical development. *J Exp Neurosci*. 12:1179069518784277.

Fazzari P, Paternain AV, Valiente M, Pla R, Lujan R, Lloyd K, Lerma J, Marin O, Rico B. 2010. Control of cortical GABA circuitry development by Nrg1 and ErbB4 signalling. *Nature*. 464:1376–1380.

Hashemi E, Ariza J, Rogers H, Noctor SC, Martinez-Cerdeno V. 2017. The number of Parvalbumin-expressing interneurons is decreased in the medial prefrontal cortex in autism. *Cereb Cortex*. 27:1931–1943.

Inan M, Welagen J, Anderson SA. 2012. Spatial and temporal bias in the mitotic origins of somatostatin- and parvalbumin-expressing interneuron subgroups and the chandelier subtype in the medial ganglionic eminence. *Cereb Cortex*. 22:820–827.

Jones EG. 1975. Varieties and distribution of non-pyramidal cells in the somatic sensory cortex of the squirrel monkey. *J Comp Neurol*. 160:205–267.

Kawaguchi Y, Kubota Y. 1997. GABAergic cell subtypes and their synaptic connections in rat frontal cortex. *Cereb Cortex*. 7:476–486.

Lim L, Mi D, Llorca A, Marin O. 2018. Development and functional diversification of cortical interneurons. *Neuron*. 100:294–313.

Markram H, Toledo-Rodriguez M, Wang Y, Gupta A, Silberberg G, Wu C. 2004. Interneurons of the neocortical inhibitory system. *Nat Rev Neurosci*. 5:793–807.

Pakkenberg B, Pelvig D, Marner L, Bundgaard MJ, Gundersen HJ, Nyengaard JR, Regeur L. 2003. Aging and the human neocortex. *Exp Gerontol*. 38:95–99.

Schwaller B, Tetko IV, Tandon P, Silveira DC, Vreugdenhil M, Henzi T, Potier MC, Celio MR, Villa AE. 2004. Parvalbumin deficiency affects network properties resulting in increased susceptibility to epileptic seizures. *Mol Cell Neurosci*. 25: 650–663.

Southwell DG, Paredes MF, Galvao RP, Jones DL, Froemke RC, Sebe JY, Alfaro-Cervello C, Tang Y, Garcia-Verdugo JM, Rubenstein JL et al. 2012. Intrinsically determined cell death of developing cortical interneurons. *Nature*. 491:109–113.

Sultan KT, Liu WA, Li ZL, Shen Z, Li Z, Zhang XJ, Dean O, Ma J, Shi SH. 2018. Progressive divisions of multipotent neural progenitors generate late-born chandelier cells in the neocortex. *Nat Commun*. 9:4595.

Sussel L, Marin O, Kimura S, Rubenstein JL. 1999. Loss of Nkx2.1 homeobox gene function results in a ventral to dorsal molecular respecification within the basal telencephalon: evidence for a transformation of the pallidum into the striatum. *Development*. 126:3359–3370.

Szentagothai J, Arbib MA. 1974. Conceptual models of neural organization. *Neurosci Res Program Bull*. 12:305–510.

Taniguchi H, Lu J, Huang ZJ. 2013. The spatial and temporal origin of chandelier cells in mouse neocortex. *Science*. 339:70–74.

Von Economo C, Koskinas G. 1928. *Cellular structure of the human cerebral cortex*. New York: Karger.

Vreugdenhil M, Jefferys JG, Celio MR, Schwaller B. 2003. Parvalbumin-deficiency facilitates repetitive IPSCs and gamma oscillations in the hippocampus. *J Neurophysiol*. 89: 1414–1422.

Wegiel J, Kuchna I, Nowicki K, Imaki H, Wegiel J, Marchi E, Ma SY, Chauhan A, Chauhan V, Bobrowicz TW et al. 2010. The neuropathology of autism: defects of neurogenesis and neuronal migration, and dysplastic changes. *Acta Neuropathol*. 119:755–770.

Wohr M, Orduz D, Gregory P, Moreno H, Khan U, Vorckel KJ, Wolfer DP, Welzl H, Gall D, Schiffmann SN et al. 2015. Lack of parvalbumin in mice leads to behavioral deficits relevant to all human autism core symptoms and related neural morphofunctional abnormalities. *Transl Psychiatry*. 5:e525.

Wong FK, Bercsenyi K, Sreenivasan V, Portales A, Fernandez-Otero M, Marin O. 2018. Pyramidal cell regulation of interneuron survival sculpts cortical networks. *Nature*. 557:668–673.

Xu Q, Tam M, Anderson SA. 2008. Fate mapping Nkx2. 1-lineage cells in the mouse telencephalon. *J Comp Neurol*. 506:16–29.